

Design and Development of a compact and efficient single-stage, transformer-less buck-boost converter for Electric vehicle chargers

¹Sampath Kumar T, ²Raja D, ³Anbumalar S, ⁴Jamina P

¹PG scholar, ^{2,3,4}Professor

Department of Electrical And Electronics Engineering, Sri managula vinayagar engineering college, Madagadipet. Puducherry.

¹Sampath.path98@gmail.com ² rajaapeee@smvec.ac.in

Abstract—Development of a single-stage, transformer-less buck-boost converter specifically designed for electric vehicle (EV) chargers. In contrast to conventional H-bridge converters, the proposed converter functions as a buck-boost DC/DC converter, offers the flexibility to establish versatile and adjustable connections between input and output voltages. This unique characteristic allows the converter to operate efficiently with flexible voltage relationships, even with peak AC output voltage exceeding DC link voltage. The design and implementation of the converter involve careful selection of power semiconductor devices with low on-state resistance and minimal switching losses. The control strategy incorporates advanced techniques like pulse width modulation (PWM) to regulate the duty cycle and ensure precise voltage and current regulation. The proposed converter's performance is evaluated through hardware and simulations, providing evidence of its effectiveness in EV charging applications. This research contributes to the advancement of power conditioning systems for EV chargers, addressing the growing demand for efficient and compact charging solutions in the electric vehicle market.

Keywords—Electrical vehicles, transformer less buck-boost converter, H-bridge converter, G2V and V2G.

I. INTRODUCTION

The conventional internal combustion (IC) engines use the products such as petrol, diesel or LPG as their source for the driving operation. Today when there is a scarcity of fossils, which is the most censorious issue around the world and has no instant cure rather minimizing its use. Moreover, the conventional internal combustion engine vehicles emit a large amount of carbon dioxide and many other greenhouse gases which makes it even more tedious job to maintain the environmental regulations. The answer to this problem entails in adopting alternative vehicles such as Hybrid Electric Vehicle (HEV) or Electric Vehicles (EV). The main advantage that an EV provide is that is do not discharge tail pipe pollutants like O₃, volatile organic components (VOC), CO, hydrocarbons, and various nitrogen oxides which play a major part in creating air pollution and causing greenhouse gases. Also, it helps in reducing the use of fossil fuels.

Electric vehicles (EVs) offer significant advantages over conventional IC-engine vehicles, including reduced environmental pollution and improved performance [1]. Plug-in hybrid electric vehicles (PHEVs) provide the convenience of charging the vehicle's battery at home or at dedicated

charging stations during parking or overnight [2]. However, there are certain limitations associated with EVs that deter some people from adopting them, such as higher initial cost compared to traditional vehicles, longer recharging times, and insufficient battery infrastructure. Power electronics devices have emerged as a solution to address these challenges by facilitating the design of EV charging stations and charger architectures, overcoming limitations and promoting the widespread adoption of EV technology.

The buck converter is employed to decrease voltage, while the boost converter is utilized to increase voltage. On the other hand, both the buck-boost and Cuk converters can handle both voltage step-down and step-up operations. In low-power applications, the charge-pump converter is employed for voltage boost or voltage reversal. The diminishing reserves of fossil fuels have led to a growing need for hybrid vehicles, which offer cost-effective, reliable, and environmentally-friendly improvements in fuel efficiency. Energy storage systems, typically in the form of battery packs, are essential components of all hybrid electric vehicles, including fuel cell vehicles.

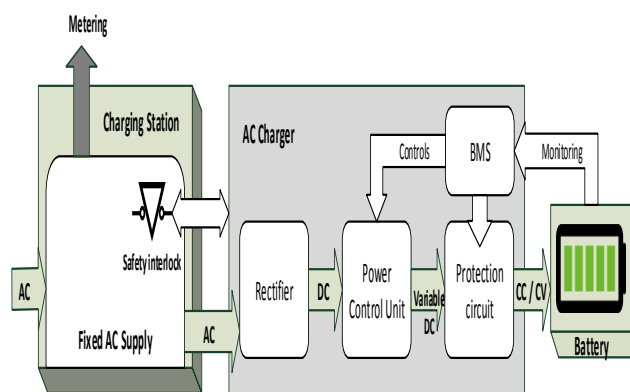


Fig. 1. Block diagram of EV vehicle charger

Battery packs encounter several challenges, including their restricted capacity to handle high current loads during regenerative braking and boost assist, potential performance degradation over time, concerns about their weight, size, and environmental implications during disposal. Electric vehicles (EVs) play a crucial role in achieving worldwide objectives to



reduce the carbon footprint caused by vehicle emissions, which contribute to climate change.

The powertrain configurations of all electric vehicles (EVs) share a common system comprised of the battery, power converter, and electric motor. Extensive research and development have been conducted on each of these components to enhance the performance of automotive traction systems. However, integrating these elements in EV applications poses significant research challenges due to their complexity.

The integration of the battery, power converter, and electric motor represents a complex interplay of technologies in EVs, necessitating ongoing research to optimize their performance. This research focuses on improving energy efficiency, extending driving range, reducing overall weight, and enhancing the overall integration and operation of these components in electric vehicles.

When cells in a battery pack are connected in series, it significantly raises the likelihood of failure within the pack. To address these challenges in the implementation of a buck-boost converter, which serves as a versatile DC-DC converter capable of adjusting the output voltage to be higher or lower than the input voltage. This converter plays a crucial role in efficiently transferring energy between the primary energy source of an electric vehicle, such as a battery pack, and an auxiliary energy system based on ultra-capacitors. By utilizing the buck-boost converter, efficient energy transfer can be achieved, allowing for optimized utilization of both the main energy source (battery pack) and the auxiliary energy system (ultra-capacitors) in electric vehicles.

II. RELATED WORK

Renewable energy sources, including wind, solar, and hydro power, have emerged as dependable substitutes for conventional energy sources like oil, natural gas, and coal. The increasing integration of Distributed Power Generation Systems (DPGSs) into the utility network has prompted the introduction of new and more stringent standards concerning power quality, safe operation, and islanding protection. Consequently, there is a growing need to ensure seamless integration with the grid, it is essential to strengthen the control mechanisms of distributed generation systems, enabling them to meet the necessary standards for grid interconnection. [1]. These advancements are necessary to maintain stable and reliable grid operations while effectively utilizing the power generated from renewable sources. By improving the control mechanisms, DPGSs can better manage the fluctuations in renewable energy generation, ensure power quality, and actively participate in grid support functions.

Grid-connected power conversion systems commonly employ high-order passive filters, such as LCL filters, to effectively mitigate switching frequency harmonics generated by power converters. Despite being smaller than conventional single-inductor L filters, passive filters such as LCL filters still tend to be bulky and expensive when compared to their active counterparts that employ semiconductor switches. In order to improve system power density and reduce costs, the magnetic integration technique has gained significant traction and

adoption. The magnetic integration technique involves replacing discrete inductors in passive filters with integrated inductors, enables the utilization of smaller magnetic cores and reduced volumes for the filters. This approach aims to improve power density and cost-effectiveness. In conventional magnetic integrated LCL filters, the integration involves combining the converter-side inductor and the grid-side inductor, while intentionally minimizing the coupling coefficient between them. This integration helps optimize the performance of the filter and achieve a more compact and efficient design, thereby addressing the limitations of traditional passive filters in terms of size and cost.

This research paper explores the utilization and design of the coupling coefficient in a magnetic integrated LCL filter. Through the integration of the inductor and the filter capacitor, the resulting coupling effect emulates the presence of an additional inductor within the filter capacitor branch loop. This integration gives rise to an integrated LLCL filter, which combines the benefits of both the LLCL filter and magnetic integration. This integrated approach offers advantages such as enhanced harmonic attenuation, decreased filter inductances, and reduced overall system volume, all without requiring an additional trap inductor. [2]. Additionally, the paper presents a stability analysis of a discrete-time domain LCL-type grid-connected inverter. The investigation demonstrates that although the system maintains stability when the resonance frequency (f_r) is higher than one-sixth of the sampling frequency ($f_s/6$), it is still crucial to employ an effective damping scheme to counteract potential influences from grid impedance. The conventional approach of using proportional capacitor-current-feedback active damping (AD) is limited to a valid damping region up to $f_s/6$.

However, it has been observed that relying solely on the conventional proportional capacitor-current-feedback active damping (AD) method is insufficient to achieve a high-quality output current in the design process. The system is susceptible to instability caused by resonance frequency shifting. To overcome this constraint and taking into account the resonance frequency design guidelines for LCL filters, this research paper presents an enhanced capacitor-current-feedback active damping (AD) method. By conducting a thorough analysis and precise parameter design, the proposed AD method extends the upper limit of the damping region to $f_s/4$, encompassing all potential resonance frequencies. This expanded damping region effectively ensures stability and resolves any potential instabilities arising from variations in the resonance frequency. The paper further investigates the effectiveness of the proposed AD method in providing damping is evaluated, assessing its effectiveness in achieving improved stability and high-quality output current [3].

The Single Ended Primary Inductance Converter (SEPIC), a widely used buck-boost topology that provides a non-inverting output. However, the SEPIC circuit has certain drawbacks, including limited efficiency and the requirement of either a transformer or two inductors [2]. The inclusion of a transformer or multiple inductors in the circuit results in increased space requirements, subsequently leading to larger size and higher costs. Additionally, the use of these

components introduces additional losses, thereby degrading the overall efficiency of the converter.

III. SINGLE STAGE TRANSFORMER LESS BUCK BOOST CONVERTER SYSTEM

To develop a new and improved charger for electric vehicles: This objective can focus on improving the charging speed, efficiency, safety, and cost-effectiveness of existing charging solutions.

To develop a new single-stage transformer less buck-boost converter with improved stability and dynamic response when operating in the Grid-to-Vehicle(G2V)mode.

To optimize the management of charging: This objective can focus on improving the management of the charging process, including scheduling and controlling the charging of multiple vehicles, and optimizing the use of available electrical capacity and grid resources.

Figure 2 illustrates the schematic diagram of the proposed single-stage transformerless buck-boost converter system. In this configuration, the constant dc-link voltage (V_{DC}) is maintained by a dedicated dc power supply. By controlling the semiconductor switches (MOSFET1-MOSFET4), the inductor (L_f) can be charged from both directions. Subsequently, the charged inductor supplies power to the filter capacitor (C_f) and the load (R) when either switch S_5 or S_6 is turned on. Within Figure 2, the variables i_L , i_R , and V_c represent the inductor current, load current, and capacitor voltage, respectively.

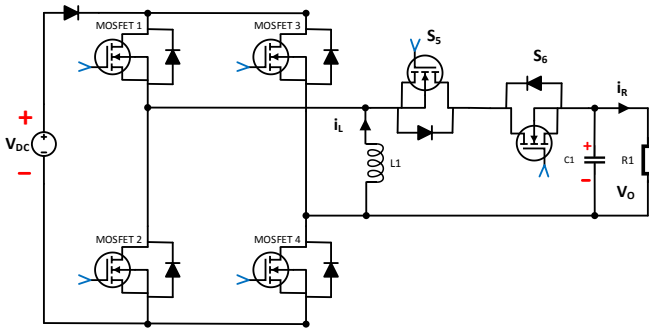


Fig. 2. Schematic design of proposed model

A. Mathematic Model

In the proposed buck-boost inverter, the following parameters are defined: T_s as the switching period, T_{on} as the switching-on time of S_2 and S_3 or S_1 and S_4 within each switching cycle, T_{off} as the switching-on time of S_5 or S_6 within each switching cycle, and d_o as the duty cycle represented by T_{on}/T_s . From Figure 2, the state equation description of the buck-boost inverter can be derived as follows.

$$\begin{bmatrix} \frac{di_L}{dt} \\ \frac{dv_C}{dt} \end{bmatrix} = \begin{bmatrix} 0 & 0 \\ 0 & \frac{-1}{R_o C_f} \end{bmatrix} \begin{bmatrix} i_L \\ v_C \end{bmatrix} + \begin{bmatrix} 1 \\ 0 \end{bmatrix} \frac{1}{L_f} v_{dc}, \quad (1)$$

$$\begin{bmatrix} \frac{di_L}{dt} \\ \frac{dv_C}{dt} \end{bmatrix} = \begin{bmatrix} 0 & \frac{-1}{L_f} \\ \frac{1}{C_f} & \frac{-1}{R_o C_f} \end{bmatrix} \begin{bmatrix} i_L \\ v_C \end{bmatrix} + \begin{bmatrix} 0 \\ 0 \end{bmatrix} v_{dc} \quad (2)$$

Equations (1) and (2) describe the switching-on and switching-off behaviors of the proposed inverter, respectively. To obtain the state space average model of the inverter, these equations can be combined with their respective weighted coefficients of d_o and $1-d_o$. By incorporating the appropriate weighted coefficients, the state space average model of the proposed inverter can be derived, providing a mathematical representation of its behavior and dynamics.

$$\begin{bmatrix} \frac{di_L}{dt} \\ \frac{dv_C}{dt} \end{bmatrix} = \begin{bmatrix} 0 & \frac{-1-d_o}{L_f} \\ \frac{1-d_o}{C_f} & \frac{-1}{R_o C_f} \end{bmatrix} \begin{bmatrix} i_L \\ v_C \end{bmatrix} + \begin{bmatrix} d_o \\ 0 \end{bmatrix} \frac{1}{L_f} v_{dc}, \quad (3)$$

Utilizing equation (3), the transfer functions from the DC-link voltage (v_{dc}) to the inductor current (i_L) and capacitor voltage (v_c) can be derived. These transfer functions describe the relationship between the input voltage and the respective output variables. A detailed analysis of the transfer functions allows for a deeper understanding of the system dynamics.

$$\frac{i_L(S)}{v_{dc}(S)} = \frac{d_o(C_f R_o S + 1)}{C_f L_f R_o S^2 + L_f S + R_o(1-d_o)^2} \quad (4)$$

$$\frac{v_C(S)}{v_{dc}(S)} = \frac{R_o d_o(1-d_o)}{C_f L_f R_o S^2 + L_f S + R_o(1-d_o)^2} \quad (5)$$

In the steady-state, equations (4) and (5) can be reorganized to provide alternative forms that enhance understanding and analysis of the system behavior.

$$\frac{I_L}{V_{dc}} = \frac{d_o}{R_o(1-d_o)^2} \quad (6)$$

$$\frac{V_c}{V_{dc}} = \frac{d_o}{1-d_o} \quad (7)$$

In the Buck-Boost converter, the output voltage (V_{out}) is set at 400V. The calculated values for the design variables are as follows: the inductor (L) is determined to be 54.48 mH, the capacitor (C) is 1.1248 μ F, and the duty cycle (D) is calculated to be 0.5624. These design variables are crucial in achieving the desired output voltage and ensuring the proper operation of the Buck-Boost converter.

It is crucial to acknowledge that equations (1)-(7) are specifically valid for positive output voltages, as illustrated in Figure 3. However, in the scenario of negative output voltages, as depicted in Figure 4, the variable V_{DC} in equations (1)-(7) should be substituted with $-V_{DC}$. This nonlinear characteristic adds complexity to controller design. To address this challenge, the absolute value of the duty cycle is employed instead of its actual value. By using the absolute value of the duty cycle, the controller can effectively handle both positive and negative output voltages, ensuring accurate and robust operation of the system.

Additionally, during the transition of the reference duty cycle from a positive value to a negative value, the driving pulses for switches MOSFET 2 and MOSFET 3 are effectively shifted to switches MOSFET 1 and MOSFET 4, respectively, and vice versa. This strategy ensures that the polarity of the output voltage (V_c) is consistently regulated to align with the sign of its reference. By implementing this approach, equations (1)-(7) remain applicable to the magnitude of the output voltage ($|V_c|$), allowing for effective control of the converter. This technique ensures proper regulation and maintains the desired behavior of the converter, enabling it to operate reliably in both positive and negative output voltage scenarios.

IV. OPERATING PRINCIPLE - SINGLE STAGE ON BOARD EV CHARGER

The operation principle of the proposed buck-boost inverter can be effectively explained by the switching patterns depicted in Figure 3 and Figure 4. Assuming that the desired waveform of the output voltage (V_c) is a sinusoid with a pulsating frequency, the behavior of the semiconductor devices is dependent on the sign of V_c . In the case of a positive half-wave of V_c , as shown in Figure 3, switches MOSFET 1 and MOSFET 4 remain in the off-state, while switch S_6 remains on, as seen in Figure 3a. Conversely, for a negative V_c , the operations of switches MOSFET 2, MOSFET 3, and S_6 are replaced by switches MOSFET 4, MOSFET 1, and S_5 , respectively.

Based on the above analysis, it can be observed that the proposed buck-boost inverter operates similarly to a conventional DC/DC buck-boost inverter, with the exception of its bipolar output voltage. As a result, it facilitates both voltage step-down and boost operations, enabling versatile functionality for the inverter.

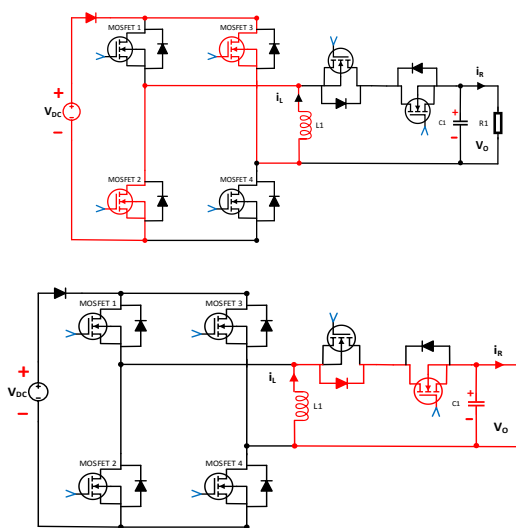


Fig. 3. Switching patterns (a) inductor charged (b) inductor discharged

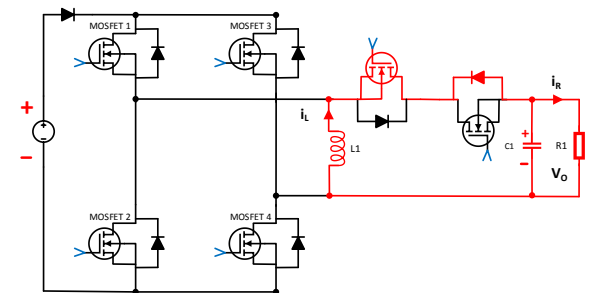
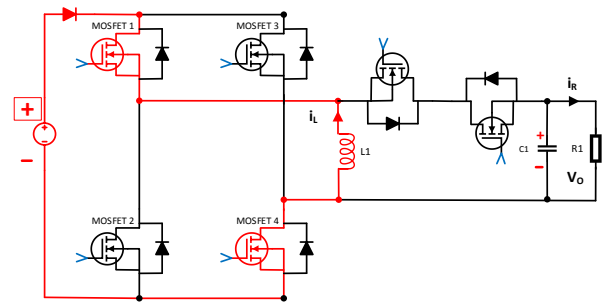


Fig. 4. Switching patterns (a) inductor charged (b) inductor discharged

The single-stage on-board EV charger incorporates an MOSFETs-based single-phase H-bridge AC-DC converter, as depicted in Figure 5. This converter possesses bidirectional capability, enabling it to perform four-quadrant operations seamlessly. The EV charger is directly linked to the single-phase AC supply through an interfacing inductor (L_s), which aids in compensating grid current harmonics and achieving a sinusoidal current waveform. On the DC side, the EV battery pack is connected in parallel with a DC link capacitor. To prevent overcharging, a control switch is placed in series with the battery pack, allowing for disconnection once the battery has reached its full charge. This design ensures efficient and reliable charging of the EV battery pack while maintaining harmonic compensation and achieving high-quality sinusoidal current output.

During the off-state, the capacitor C_1 discharges its energy to provide power to the load R_1 . Conversely, as illustrated in Figure 7, it is evident that the inductor L_f transfers its energy to the capacitor C_1 and the load R_1 when switches MOSFET 2 and MOSFET 3 are turned off, while switch S_6 is turned on. When switches MOSFET 2 and MOSFET 3 turn on, the DC power supply charges the inductor L_1 . Consequently, the inductor current i_L exhibits a linear increase as a result of this charging process. This behavior demonstrates the dynamic energy transfer within the system, wherein the inductor and capacitor exchange energy to effectively supply power to the load and maintain a continuous and controlled operation.

The single-phase AC-DC converter possesses an inherent characteristic of generating a periodic second-order ripple on the DC side. This ripple can be further amplified by periodic

disturbances or noise present in the input AC supply. The presence of this double-frequency ripple component on the DC side can lead to increased ripple in battery voltage and current, ultimately impacting the lifetime of the battery.

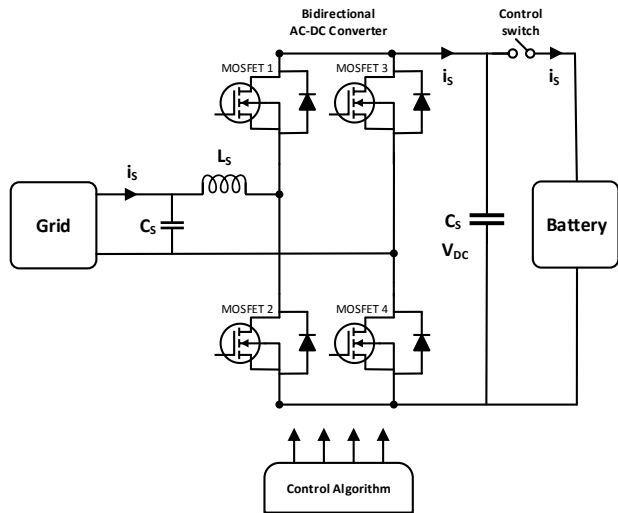


Fig. 5. Single stage on board EV charger

This phenomenon highlights the importance of addressing ripple reduction techniques in the design of the converter. By implementing appropriate filtering and control strategies, the adverse effects of ripple can be minimized, thereby improving the overall performance and longevity of the battery in the system.

V. SIMULATION AND HARDWARE RESULTS

To validate the presented DC-DC converter based on the single-stage quadratic voltage gain buck-boost topology, a proof-of-concept test bench prototype was developed and implemented in a laboratory setting. A photograph of the test bench setup can be observed in Figure 6. This prototype serves as a tangible demonstration of the converter's functionality and performance in a real-world environment. The test bench provides a practical platform for conducting experiments, gathering data, and evaluating the converter's behavior, thereby confirming the feasibility and practicality of the proposed design.

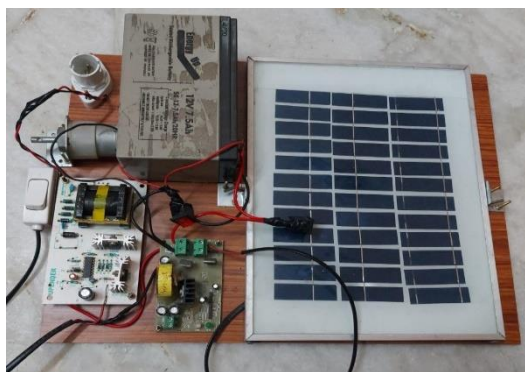


Fig. 6. Hardware Setup of single stage transformer less buck boost converter

Figure 7 shows that the simulation results of buck boost converter for the battery charging and discharging. It displays the waveforms for a steady state response of dc-dc converter at charging when higher side voltage is low and lower side voltage is high at that time higher side battery is charging from 30% of battery charging and lower side battery discharging from 80 % of charge. Battery charging voltage and discharging voltage is shown in Figure 7 and percentage of battery charging and discharging is shown in Figure 8.

The proposed EV charger and its control system are simulated using MATLAB/Simulink. The primary objective of this research is to develop a robust control system for a single-phase, single-stage EV charger that can operate effectively in a wide range of Grid-to-Vehicle (G2V) and Vehicle-to-Grid (V2G) modes. A key focus of the control system design is to minimize the impact of the second-order ripple current component on the DC side.

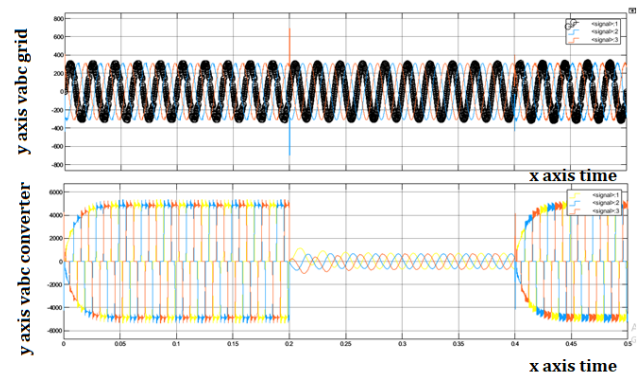


Fig. 7. Current Response of buck boost converter

Through the simulation, various control strategies and algorithms are evaluated to ensure the charger's reliable and efficient operation under different operating conditions. The goal is to optimize the charger's performance while reducing the undesired ripple current component, which can have detrimental effects on battery life and overall system efficiency. By implementing a robust control system, the proposed EV charger aims to enhance the user experience, maximize charging efficiency, and support bi-directional power flow in grid-connected applications.

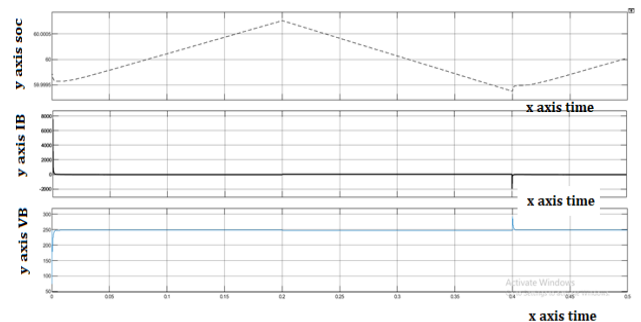


Fig. 8. Battery charging and discharging

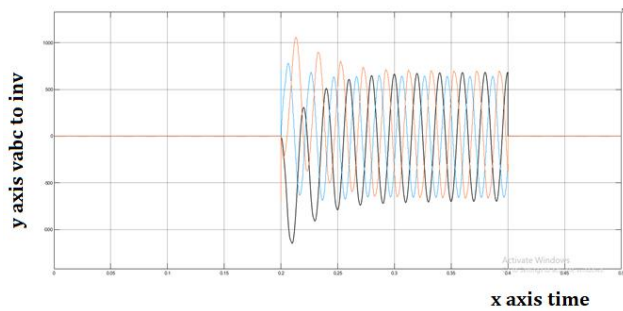


Fig. 9. V2G and G2V mode of operations

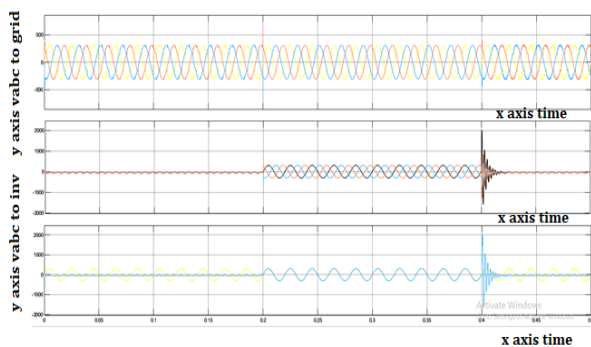


Fig. 10. G2V and V2G mode of operations

This graph shows the amount of voltage and current being charged into or discharged from an EV's battery over time. It is understood that during change over from the charging and discharging, there is peak rise voltage and current. Thus patterns of EV charging and the potential for G2V and V2G mode of operations are determined.

VI. CONCLUSIONS

This project introduces an innovative solution known as the single-stage transformerless buck-boost converter, which enables direct DC-to-DC conversion regardless of the relationship between the DC-link voltage and the peak AC output voltage. This converter presents several advantages over conventional boost converters, including a simplified circuit structure, reduced cost, smaller physical size, and straightforward implementation. The stability analysis of the proposed converter, based on its state-space average model, reveals that stability is influenced by the duty cycle value. However, this challenge can be effectively addressed through the implementation of a well-designed controller that incorporates an outer voltage-loop and an inner current-loop. These control mechanisms ensure stable operation and precise regulation of the converter. Simulation results are presented to validate the performance and stability of the proposed converter. These simulations provide evidence of its effectiveness in achieving the desired output performance, confirming its potential as a reliable and efficient solution for DC-to-DC conversion in various applications.

The efficiency of the electric vehicle chargers calculated to a value of 91.60% which is testified through simulation results. Further a detailed tabulated comparison of this converter with six different topologies has been presented. The criteria for selection of these topologies are the number of

inputs and outputs. The comparison is based on five different features in which the major characteristic considered is the Part Count as it directly affects the efficiency of the converter. The DC-DC converter in this project has only five i.e. minimum numbers of primary components namely an inductor, a capacitor and three switches, thereby having a high efficiency. Along with the MATLAB simulation, the fabrication of the Converter has also been carried out.

REFERENCES

- [1] Blaabjerg, F.; Teodorescu, R.; Liserre, M.; Timbus, A.V. Overview of control and grid synchronization for distributed power generation systems. *IEEE Trans. Ind. Electron.* 2006, 53, 1398–1409. [CrossRef]
- [2] Fang, J.; Li, H.; Tang, Y. A magnetic integrated LLCL filter for grid-connected voltage-source converters. *IEEE Trans. Power Electron.* 2017, 32, 1725–1730. [CrossRef]
- [3] Li, X.; Wu, X.; Geng, Y.; Yuan, X.; Xia, C.; Zhang, X. Wide damping region for LCL-type grid-connected inverter with an improved capacitor-current-feedback method. *IEEE Trans. Power Electron.* 2015, 30, 5247–5259. [CrossRef]
- [4] Fang, J.; Li, X.; Yang, X.; Tang, Y. An integrated trap-LCL filter with reduced current harmonics for grid-connected converters under weak grid conditions. *IEEE Trans. Power Electron.* 2017, 32, 8446–8457. [CrossRef]
- [5] Li, X.; Fang, J.; Tang, Y.; Wu, X.; Geng, Y. Capacitor voltage feedforward with full delay compensation to improve weak grids adaptability of LCL-filtered grid-connected converters for distributed generation systems. *IEEE Trans. Power Electron.* 2018, 33, 749–764. [CrossRef]
- [6] Tang, Y.; Loh, P.C.; Wang, P.; Choo, F.H.; Gao, F.; Blaabjerg, F. Generalized design of high performance shunt active power filter with output LCL filter. *IEEE Trans. Ind. Electron.* 2012, 59, 1443–1452. [CrossRef]
- [7] Fang, J.; Xiao, G.; Yang, X.; Tang, Y. Parameter design of a novel series-parallel-resonant LCL filter for single-phase half-bridge active power filters. *IEEE Trans. Power Electron.* 2017, 32, 200–217. [CrossRef]
- [8] Fang, J.; Li, X.; Tang, Y. A novel LCL-filtered single-phase half-bridge distributed static compensator with dc-link filter capacitors and reduced passive component parameters. In *Proceedings of the IEEE Applied Power Electronics Conference and Exposition (APEC)*, Tampa, FL, USA, 26–30 March 2017; pp. 3279–3285.
- [9] Yang, S.; Wang, P.; Tang, Y.; Zhang, L. Explicit phase lead filter design in repetitive control for voltage harmonic mitigation of VSI-based islanded microgrids. *IEEE Trans. Ind. Electron.* 2017, 64, 817–826. [CrossRef]
- [10] Delille, G.; Francois, B.; Malarange, G. Dynamic frequency control support by energy storage to reduce the impact of wind and solar generation on isolated power system's inertia. *IEEE Trans. Sustain. Energy* 2012, 3, 931–939. [CrossRef]
- [11] Emadi, A.; Williamson, S.S.; Khaligh, A. Power electronics intensive solutions for advanced electric, hybrid electric, and fuel cell vehicular power systems. *IEEE Trans. Power Electron.* 2006, 21, 567–577. [CrossRef]
- [12] Yilmaz, M.; Krein, P.T. Review of battery charger topologies, charging power levels, and infrastructure for plug-in electric and hybrid vehicles. *IEEE Trans. Power Electron.* 2013, 28, 2151–2169. [CrossRef]
- [13] Fang, J.; Xiao, G.; Xu, Y.; Tang, Y. An optimal digital pulse-width-modulated dither technique to enhance the resolution of high frequency power converters. *IEEE Trans. Power Electron.* 2017, 32, 7222–7232. [CrossRef]
- [14] Peng, F. Z-source inverter. *IEEE Trans. Ind. Appl.* 2003, 39, 504–510. [CrossRef]
- [15] Fang, J.; Xiao, G.; Zhang, Y. An LCCL filter and its application to a half-bridge APF. In *Proceedings of the 9th International Conference on Power Electronics and ECCE Asia (ICPE-ECCE Asia)*, Seoul, Korea, 1–5 June 2015; pp. 2566–2.



- [16] Fang, J.; Li, X.; Tang, Y. "A review of passive power filters for voltage-source converters". In Proceedings of the 2016 Asian Conference on Energy, Power and Transportation Electrification (ACEPT), Singapore, 25–27 October 2016.
- [17] Ravishankar A. N, Kumaravel S., Ashok S., "Bidirectional Dual Input Single Output DC-DC Converter for Electric Vehicle Charger Application", 2019 IEEE 8th Global Conference on Consumer Electronics (GCCE)
- [18] SajibChakrabortya, HaarisRasool, Dai-Duong Tran, Thomas Geury, Mohamed El Baghdadi, Omar Hegazy, "Design and Implementation of a Multifunctional 6-phase Interleaved Bidirectional DC/DC Converter for Battery Electric Vehicle Applications", IEEE Conference Publication, IEEE Xplore, ISBN:978-9-0758-1537-5.
- [19] ShokoufehValadkhani, Mojtaba Mirsalim, Gevork B. Gharehpetian "Bidirectional Isolated DC/DC Dual-Active-Bridge Converters Optimum Soft-Switching Control Method for Electrical Vehicle Applications", IEEE Conference Publication, IEEE Xplore, 978-1-6654-3365-5.
- [20] ArkaBasu and Subhajyoti Mukherjee, "Analysis and Design of a Multiport Converter based Integrated On-board Charger for Electric Vehicle Powertrains", IEEE Conference Publication, IEEE Xplore, 978-1-7281-5135-9.